Effect of reaction time on the structure and optical properties of P3HT/MWCNT-OH nanocomposites

Mohd Nurazzi Norizan[1] (ORCID ID: 0000-0001-7697-0511), **Norli Abdullah**[1, *] (0000-0002-8519-3379), **Siti Zulaikha Ngah Demon**[1] (0000-0001-6706-7216), **Norhana Abdul Halim**[1] (0000-0001-8077-824X), **Nurul Syahirah Nasuha Sa'aya**[1], **Imran Syakir Mohamad**[2] (0000-0002-3805-9919)

DOI: dx.doi.org/10.14314/polimery.2022.5.3

Abstract: In the present study, regioregular poly(3-hexylthiophene-2,5-diyl) (P3HT) coated hydroxylated multi-walled carbon nanotubes (MWCNT-OH) nanocomposites were prepared over different reaction times of non-covalent functionalization. The reaction time was set as 24, 48, 72, 96, and 120 hours. The structure and optical characteristics of nanocomposites were analyzed using Fourier-transform infrared (FTIR) and ultraviolet-visible (UV-Vis) spectroscopy, respectively. Reaction time affected prepared nanocomposites by decreasing the intensity of the P3HT/MWCNT-OH peaks gradually with increasing of the reaction time. Comparing with the pure P3HT and MWCNT-OH, the calculated energy band gap and the Urbach energy of the nanocomposites were reduced proportionally as the reaction time reached 120 hours and achieved 2.60 and 0.329 eV, respectively.

Keywords: carbon nanotubes, energy band gap, P3HT, MWCNT-OH, UV-Vis, FTIR, Urbach energy.

Wpływ czasu reakcji na strukturę i właściwości optyczne nanokompozytów P3HT/MWCNT-OH

Streszczenie: Syntetyzowano hydroksylowane wielościenne nanorurki węglowe (MWCNT-OH) pokryte stereoregularnym poli(3-heksylotiofen-2,5-diylu) (P3HT) oraz zbadano wpływ czasu reakcji niekowalencyjnej funkcjonalizacji na strukturę i właściwości optyczne otrzymanego nanokompozytu. Czas reakcji wynosił 24, 48, 72, 96 i 120 godzin. W badaniach wykorzystano spektroskopię w podczerwieni z transformacją Fouriera (FTIR) oraz ultrafioletową UV-Vis. Wraz ze wzrostem czasu reakcji następowało stopniowe zmniejszenie intensywności pików P3HT/MWCNT-OH. W porównaniu z P3HT i MWCNT-OH obliczona przerwa energetyczna i energia Urbacha zmniejszały się wraz z wydłużeniem czasu reakcji i osiągnęły odpowiednio 2,60 i 0,329 eV przy czasie reakcji 120 godzin.

Słowa kluczowe: nanorurki węglowe, przerwa energetyczna, P3HT, MWCNT-OH, UV-Vis, FTIR, energia Urbacha.

Poly(3-hexylthiophene-2,5-diyl) (P3HT) is a semiconducting organic macromolecule and excellent conductive polymer used as an electron donor for organic solar cells. The compound consists of sulfur heterocycles polymerized through the 2,5-positions with head-to-head substitution [1]. P3HT is the most widely used *p*-type donor material. Nevertheless, a significant energy band gap between 2.0 and 3.5 eV and a relatively high HOMO (highest occupied molecular orbital) energy level at approximately 5.0 eV are the limitations associated with P3HT [2, 3]. The maximum flux density of a solar spectrum was recorded at around 700 nm or 1.7 eV. A higher energy band gap hampers efficient absorption of most solar radiations (red and infrared regions), which is the primary reason for the reduced efficiency of P3HT. Nonetheless, the absorption energy efficiency of P3HT could be improved by reducing the energy band gap via hybridization with *n*-type carbon nanotubes (CNTs) [4]. Furthermore, *p*-*n* heterojunctions with semiconductor materials allow modification, hence permitting manipulation of absorption intensity capabilities of the conductive materials by altering the electrical performance around the hetero-interfaces [5].

The CNTs have gained attention as the reinforcement substance in numerous nanomaterials issues due to their low cost, mechanical stability, high aspect ratio, excellent thermal and electronic conductivity, tunable carbon framework, and hollow and layered nanosized structure

[1] Centre for Defence Foundation Studies, National Defence University of Malaysia, Kem Sungai Besi, 57000 Kuala Lumpur, Malaysia.

[2] Faculty of Mechanical Engineering, Universiti Teknikal Malaysia Melaka, Hang Tuah Jaya, 76100 Durian Tunggal, Melaka, Malaysia.

[*] Author for correspondence: norli.abdullah@upnm.edu.my

[6–8]. The CNTs possess remarkable prospect for applications in several scientific and technological fields, especially as nanocomposite fillers in polymers where the addition of CNTs enhances the mechanical, thermal, and electrical performance of the fabricated nanocomposites. Other implementations of CNTs include microwave absorption [9, 10], batteries [11, 12], natural fiber reinforced composites [13, 14], electromagnetic interference shielding (EMI) [15, 16], corrosion protection [17, 18], solar cells [19–22], chemical sensor [23–29], hydrogen storage [30, 31], and field-emission materials [32, 33].

Pristine CNTs could not be processed as dispersion and dissolving the nanotubes in volatile organic solvents (VOS) or polymeric matrices is laborious due to rigidity, chemical inertness, and strong π-π interactions. Commercial CNTs tend to agglomerate in bundles or entanglements comprising of fifty to a few hundred of individual CNTs held together by van der Waals forces [34, 35]. The physical nature of the CNTs particles also affects their dispersion in a polymer matrix. The bundling and agglomeration of CNTs deteriorated the mechanical and electrical performance of nanocomposites compared to the theoretical predictions of individual CNTs [36–38]. Accordingly, incorporating individual CNTs, relatively smaller bundles, or disentangled CNTs wrapped and functionalized with desired polymer matrix presents a challenge.

The dispersion of CNTs is a geometrical problem arising from the length and size of the CNTs. Separating individual CNTs from agglomerates and stabilizing them in a polymer matrix is another issue. Segregating the CNTs is necessary to avoid secondary agglomeration and high entanglement. Moreover, highly efficient π-conjugated systems might enable the movements of charge carriers in nanocomposites, resulting in a significantly enhanced direct current (DC) electrical conductivity, electrochemical characteristics, sensing efficiencies, and limit of detection (LOD) [39].

Non-covalent functionalization is preferred as several CNTs applications are incompatible with covalent modification. Moreover, the technique provides better dispersion of CNTs and polymers. According to Zhao *et al.*, non-covalent functionalization with small molecules and grafting or coating nanotubes with polymers, could also alter the electrochemical properties of the nanocomposite itself [40]. Although surface defects due to functionalization from certain functional groups might reduce the performance of the nanocomposites, the method is still desirable due to the possibility of adsorbing various groups of ordered structures on the CNTs surfaces without disturbing the extended *p*-conjugations of the nanotubes. Additionally, the non-covalent functionalization approach is preferred to wrap the sidewalls of CNTs in desired polymer matrices. Consequently, the present study investigated the effects of reaction time on the structural and optical properties of poly(3-hexylthiophene-2,5-diyl) (P3HT) wrapped hydroxylated multi-walled carbon nanotubes (MWCNT-OH) via non-covalent functionalization. Analyses were performed using FTIR and UV-Vis.

EXPERIMENTAL PART

Materials

Commercially available MWCNT-OH (purity >95%) was purchased from GetNanoMaterials Malaysia. Regioregular P3HT [50,000 to 100,000 molecular weight (M_w) and ≥90% purity] were purchased from Sigma-Aldrich, United States. The organic solvent, tetrahydrofuran (THF) and methanol (CH_3OH) were purchased from Sigma Aldrich, Malaysia. All materials and solvent were used as received without further purification.

Preparation of P3HT/MWCNT-OH nanocomposites

10 mg of P3HT and 10 mg of MWCNT-OH were added to a 25 ml volumetric flask with a magnetic bar before pouring 10 ml THF. The volumetric flask was then placed on a ceramic heating plate and the mixture was stirred at 650 rpm and 50°C for 24 hours. Subsequently, the reaction mixture in the volumetric flask was sonicated at a frequency of 50 Hz for 2 hours. The temperature of the water bath sonicator was maintained between 25°C to 30°C and controlled with the addition of an ice cube. The resultant P3HT/MWCNT-OH nanocomposite (mixture color: dark olive green) precipitate was then carefully washed several times with methanol (turning to light purple) and filtered with a vacuum Buchner funnel. Finally, the obtained black powder was dried at room temperature for 24 hours. The procedure was repeated with the same amount of materials at different reaction times of 48, 72, 96, and 120 hours.

Characterization of nanocomposite samples

Structural analysis of the prepared nanocomposites was performed using Perkin Elmer Frontier spectrometer FTIR within the 500 cm^{-1} to 4500 cm^{-1} scanning range and 16 scan numbers. The P3HT/MWCNT-OH nanocomposites were mixed with potassium bromide (KBr) pellets at a 1 : 9 ratio to obtain a better resolution. For optical performance, UV-3600i Plus UV-Vis-NIR spectrophotometer from Shimadzu was used to conduct the UV-Vis diffuse reflectance spectra analysis, operating on a wavelength between 200 nm to 800 nm.

RESULTS AND DISCUSSION

FTIR analysis

Figure 1 illustrates the FTIR spectra reflecting changes in chemical structures of the P3HT/MWCNT-OH. The P3HT exhibited sharp bands at 2917 cm^{-1} and 2850 cm^{-1} corresponding to -C-H_2 stretching vibration and at 3056 cm^{-1} attributable to -C-H_3 asymmetrical stretching vibration. The bands observed at 1455 cm^{-1} and 1509 cm^{-1} were assigned to the symmetric C=C and asymmetric stretching vibrations, respectively, while the band at

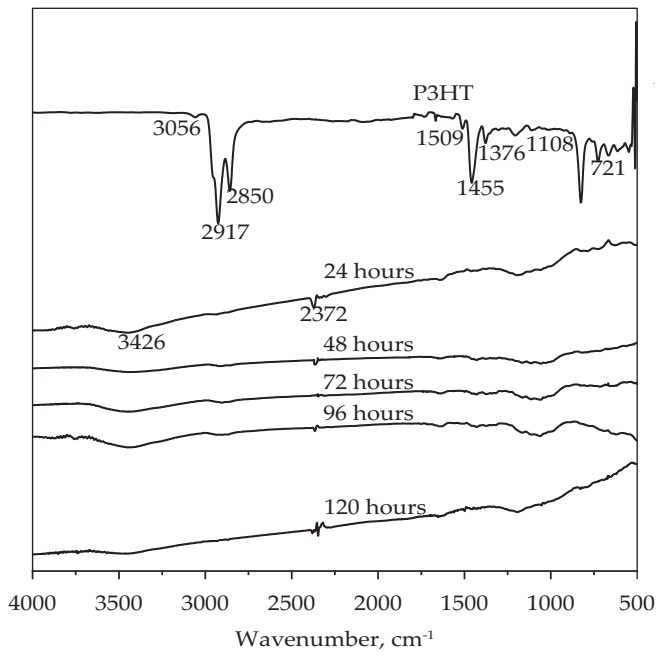

Fig. 1. FTIR spectra of the P3HT and P3HT/MWCNT-OH nanocomposite obtained at different reaction time

1376 cm^{-1} denoted the bending vibration mode of -C-H_3. The bands observed at 1108 cm^{-1} might correspond to the -C-H out of plane bending vibration of the P3HT ring. The band observed at 721 cm^{-1} was assigned to -C-H strain mode outside the plane of the 2,5-substituted thiophene ring, while the band observed at 661 cm^{-1} was denoted to the C-S bending mode [41, 42]. The P3HT/MWCNT-OH nanocomposites FTIR spectra exhibited almost identical bands to the P3HT. The new bands observed at 3426 cm^{-1} and 2372 cm^{-1} referred to the -OH stretching vibration and -C-O bond from the MWCNT-OH structure. Moreover, the intensity of the P3HT/MWCNT-OH peaks gradually decreased with increasing the reaction time. The finding might be due to the interfacial entrapment and coating of the MWCNT-OH surfaces with P3HT macromolecules.

UV-Vis analysis

The UV-Vis spectra of the P3HT/MWCNT-OH nanocomposites are shown in Figure 2. An absorption band of the pristine P3HT was observed at 556.5 nm, referring to the π-π* electronic transition of its conjugated segments. A broad band recorded at 613.5 nm was associated with the n-π*. The absorption band values were in line with previous studies [43, 44]. Nevertheless, other reports, which employed thiophene monomers to prepare P3HT instead of commercially available P3HT, documented absorption bands at approximately 495 nm [45], 456 nm [46], 308 nm [47], and 478 nm to 444 nm [48].

The π-π* and n-π* absorption bands of the P3HT/MWCNT-OH nanocomposites prepared at different reaction times in the current study demonstrated gradual shifts towards higher wavelength values, from 566.5 nm to 581 nm and from 615 nm to 623.5 nm. The observation suggested a decreased band gap and increased conjugation length [44] due to the prolonged reaction time. The longer reaction time resulted in an extended interaction between the P3HT and the MWCNT-OH. Furthermore, prolonged reaction time might uncoil and reduce the agglomerations of MWCNT, hence elevating the P3HT coating effectiveness due to the higher MWCNT-OH surface area.

Figure 2 illustrates the π-π* absorption peak intensities of the nanocomposites prepared, demonstrating elevated intensity with increasing of reaction time from 3.00 (24 hours) to 3.40 (120 hours). Whereas, the n-π* adsorption peak intensity was increased from 3.10 (24 hours) to 3.56 (120 hours). The data indicated that the P3HT π-conjugation was improved, resulting from the well-organized linkages created by the electronic transition of the P3HT and MWCNT-OH [49].

In the present study, the optical band gap of the prepared nanocomposites was calculated according to the Tauc relation (Eq. 1) from the linear part of the UV-Vis spectra at the absorption edge. The power coefficient, n, in the equation determined the possible electronic transitions during absorption processes [50] or direct band transition of the nanocomposites at $n = 1/2$. The direct band gap was attained from extrapolating the straight portion of the plot on the $h\nu$ axis at $\alpha = 0$.

$$\alpha h\nu = A(h\nu - E_g)^n \quad (1)$$

where:
E_g – optical band gap
α – absorption coefficient
hν – incident photon energy
A – constant.

The energy band gap of the P3HT and P3HT/MWCNT-OH nanocomposites prepared at different reaction times is shown in Figure 3 and Table 1. The energy band gap was reduced from 3.47 eV (P3HT) to 2.60 eV (nanocomposite obtained after 120 hours), which could be assigned to the better interaction of MWCNT-OH with P3HT. The results demonstrated that prolonged reaction time improved the coating effectiveness of the P3HT on the MWCNT-OH sidewall. Consequently, the phenomenon enhanced the π-conjugated backbone of P3HT on the MWCNT-OH sidewall, elevating the π-delocalization effects and reducing the energy band gap of the nanocomposites [4, 51, 52].

Urbach energy

According to Bafandeh *et al*. [55], due to structural disorder in amorphous materials, dense and localized state might exist between the valence and conduction bands. The phenomenon is known as Urbach energy (E_u) or Urbach tail. The E_u indicates the width of the exponen-

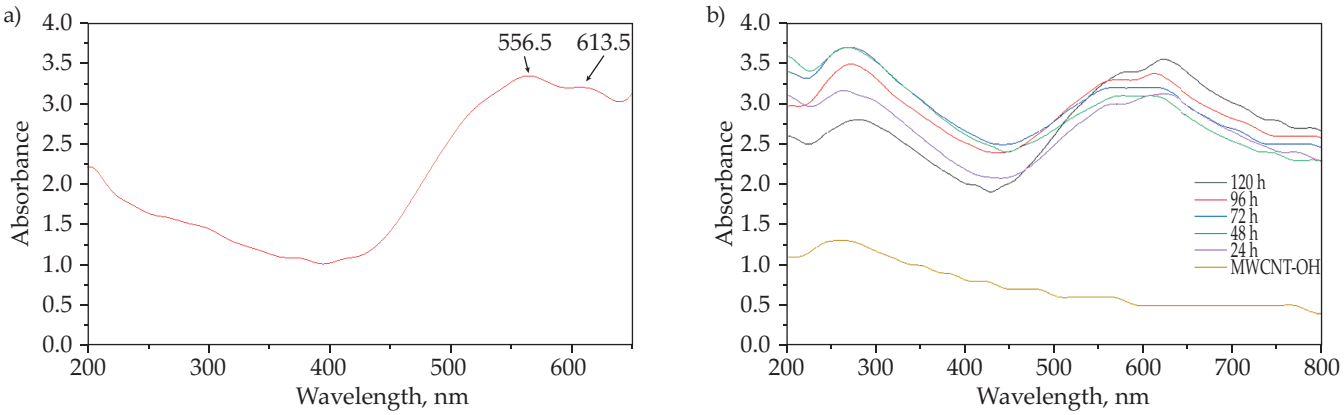

Fig. 2. UV-Vis spectra of the nanocomposites obtained at different reaction time: a) P3HT and b) P3HT/MWCNT-OH nanocomposites

tial absorption due to band tailing, which influences the energy band gap. Its value also demonstrates the disorder grade in the amorphous structure [58]. Commonly, in a disordered medium, as in the case of the hybrid P3HT/MWCNT-OH structure prepared in the present study, transitions could be induced between extended states of the valence band and localized states of the conduction band. In this situation, the corresponding state densities spread in the band gap with E_u, resulting in a tail on the absorption spectrum called the Urbach tail that possesses higher energy than the band gap. The absorption coefficient is described by the Urbach energy amounts, represented by Eq. 2.

$$\alpha(h\nu) = \alpha_0 \exp(h\nu/E_u) \quad (2)$$

where:
α_0 – positive constant
E_u – width of the Urbach tail.

The width of the localized states (band tail energy or E_u) could be estimated from the $\ln\alpha(h\nu)$ slope of composite films in the linear part, and the Urbach energy is the inverse of this slope (see Figure 4). The E_u values of the P3HT/WMCNT-OH synthesized at different reaction times are summarized in Table 1. The E_u of the pristine P3HT and MWCNT-OH were 0.392 and 0.389, respectively. The energy decreased with increasing the reaction time with the maximum value of the P3HT/MWCNT-OH nanocomposites being 0.329 eV.

Table 1 demonstrates the comparison between the E_u and energy band gap values, indicating similar behavior with an increasing reaction time. The data showed that the E_u was reduced with a longer reaction time, suggesting improved homogeneity and atomic-scale dispersion induced by well-distributed MWCNT-OH and P3HT coating incorporation in the nanocomposite. Based on findings done by Anyaegbunam and Augustine [59], the decrease in the optical band gap with precursor concentration may be attributed to the increase in grain size and

T a b l e 1. Energy band gap of the P3HT, prepared P3HT/MWCNT-OH, and other conductive nanocomposites

Sample		Energy band gap, eV	Urbach energy, eV	Reference
P3HT		3.47	0.392	The present study
MWCNT-OH		3.04	0.389	
P3HT/ MWCNT-OH	24 hours	2.82	0.352	
	48 hours	2.79	0.285	
	72 hours	2.77	0.263	
	96 hours	2.63	0.270	
	120 hours	2.60	0.329	
PANI		3.56	–	[53]
PANI/GO		2.87		
PANI/MWCNT (15 wt%)		1.78		[54]
PANI/MWCNT (4 wt%)		3.29		[55]
PPy		3.1		[56]
PEDOT		1.1		
PPy/MWCNT-COOH		2.6		[57]

Note: PPy – polypyrrole, PANI – polyaniline, PEDOT – poly(3,4-ethylenedioxythiophene), MWCNT-COOH – carboxylated multi-walled carbon nanotubes, GO – graphene oxide.

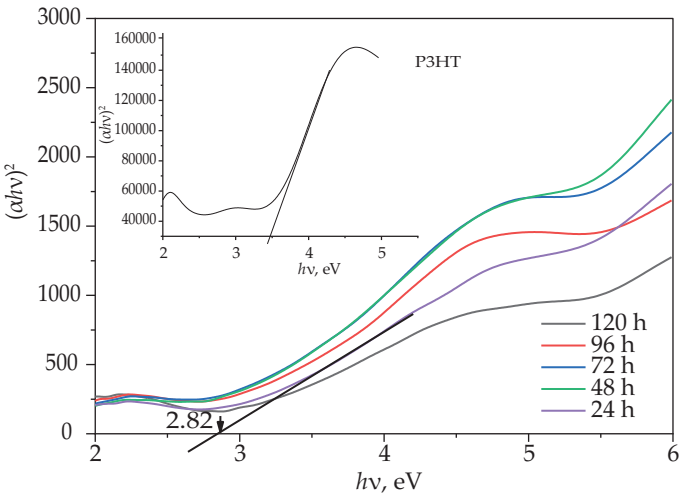

Fig. 3. Energy band gap of the P3HT and P3HT/MWCNT-OH nanocomposites obtained at different reaction time

decrease in structural disorder in the nanocomposite films as observed from Urbach energy analysis. Their results concluded that the decreased Urbach energy decreased the disordered structure of the amorphous materials [59]. They proved that as the reaction time was prolonged, the influence of tailing on the energy band gap was hindered. Another study documented that the E_u was elevated as the energy band gap decreased due to a dense localized state between valence and conduction bands [55].

CONCLUSIONS

The effect of reaction time (24, 48, 72, 96, and 120 hours) on the structural and optical properties of P3HT/MWCNT-OH nanocomposites was evaluated in the present study. The UV-Vis spectra presented two absorbance peaks related to P3HT in all the nanocomposite samples. The energy band gap value decreased with increasing of reaction time, denoting the rise of localized states in P3HT chains and the π–π* electron interactions between the P3HT and MWCNT-OH. The calculated Urbach energy of E_u was reduced with a longer reaction time, suggesting the importance of the homogeneous disorder, atomic-scale dispersion and due to the rise of localized state formation in polymer chains induced by well-distributed MWCNT-OH and P3HT coating. Therefore, understanding the effect of P3HT wrapped MWCNT-OH based on different reaction times may be helpful in designing and synthesis of the nanocomposites and the use of the best reaction time that allows for achieving the desired functionalization of elements and optimum structure of nanocomposites with targetted results. Such a detailed understanding of the effect of P3HT wrapped MWCNT-OH based on different reaction times on the structural and optical properties may also help in the designing and synthesis of novel polymer nanocomposites materials for photovoltaic devices, chemical sensors, and other electronic devices.

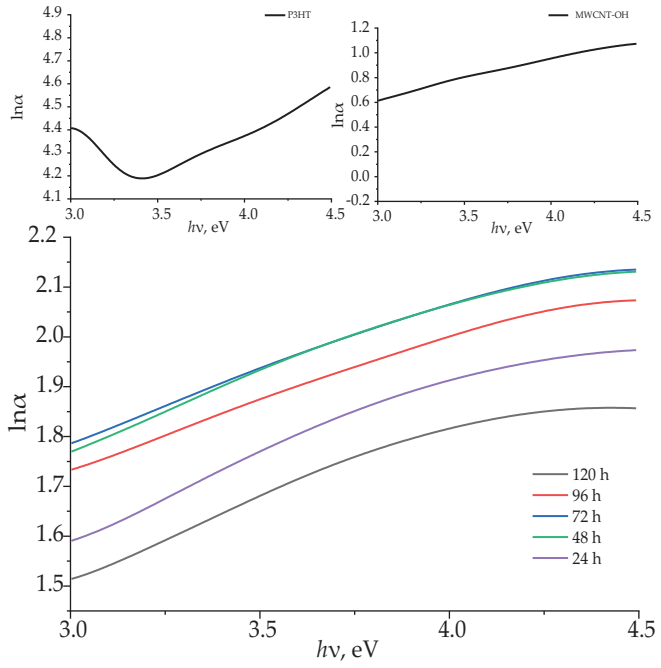

Fig. 4. E_u of synthesized P3HT/MWCNT-OH nanocomposites

ACKNOWLEDGEMENT

Financial support from Department of Higher Education (JPT), Ministry of Higher Education Malaysia and The Science and Technology Facilities Council, United Kingdom (STFC) under Newton fund's Program and Malaysia Partnership and Alliances in Research (MyPAiR) for research grant ISIS-NEWTON/2019/SG/01 and Chemical Defence Research Centre (CHEMDEF), National Defence University of Malaysia for a research grant UPNM/2018/CHEMDEFF/ST/3 are gratefully acknowledged.

REFERENCES

[1] Yang C., Zhang S., Hou J.: *Aggregate* **2021**:e111. https://doi.org/10.1002/agt2.111

[2] Tsai H.W., Hsueh K.L., Chen M.H., Hong C.W.: *Crystals* **2021**, *11*(*11*), 1292. https://doi.org/10.3390/cryst11111292

[3] Nurazzi N.M., Harussani M.M., Demon S.Z. *et al.*: *ZULFAQAR Journal of Defence Science, Engineering and Technology* **2022**, *5*(*1*). https://zulfaqarjdset.upnm.edu.my/index.php/zjdset/article/view/65

[4] Ansari M.A., Mohiuddin S., Kandemirli F., Malik M.I.: *RSC Advances* **2018**, *8*(*15*), 8319. https://doi.org/10.1039/C8RA00555A

[5] Hu Q., Lu Z., Wang Y. *et al.*: *Journal of Materials Chemistry A* **2020**, *8*(*26*), 13095. https://doi.org/10.1039/D0TA03247F

[6] Norizan M.N., Moklis M.H., Demon S.Z. *et al.*: *RSC Advances* **2020**, *10*(*71*), 43704. https://doi.org/10.1039/D0RA09438B

[7] Mohd Nurazzi N., Asyraf M.M., Khalina A. *et al.*: Polymers **2021**, *13*(*7*), 1047. https://doi.org/10.3390/polym13071047

[8] Nurazzi N.M., Abdullah N., Demon S.Z. *et al*.: *Nanotechnology Reviews* **2021**, *10*(*1*), 330. https://doi.org/10.1515/ntrev-2021-0030
[9] Wu Z., Yang Z., Pei K. *et al*.: *Nanoscale* **2020**, *12*(*18*), 10149. https://doi.org/10.1039/D0NR01447H
[10] Mo Z., Yang R., Lu D. *et al*.: *Carbon* **2019**, *144*, 433. https://doi.org/10.1016/j.carbon.2018.12.064
[11] Chen M., Jing Q.S., Sun H.B. *et al*.: *Langmuir* **2019**, *35*(*19*), 6321. https://doi.org/10.1021/acs.langmuir.9b00558
[12] Guo F., Kang T., Liu Z. *et al*.: *Nano Letters* **2019**, *19*(*9*), 6377. https://doi.org/10.1021/acs.nanolett.9b02560
[13] Medupin R.O., Abubakre O.K., Abdulkareem A.S. *et al*.: *Scientific Reports* **2019**, *9*(*1*), 1. https://doi.org/10.1038/s41598-019-56778-0
[14] Abidin M.S., Herceg T., Greenhalgh E.S. *et al*.: *Composites Science and Technology* **2019**, *170*, 85. https://doi.org/10.1016/j.compscitech.2018.11.017
[15] Feng D., Xu D., Wang Q., Liu P.: *Journal of Materials Chemistry C* **2019**, *7*(*26*), 7938. https://doi.org/10.1039/C9TC02311A
[16] Zhou E., Xi J., Guo Y. *et al*.: *Carbon* **2018**, *133*, 316. https://doi.org/10.1016/j.carbon.2018.03.023
[17] Souto L.F., Soares B.G.: *Progress in Organic Coatings* **2020**, *143*, 105598. https://doi.org/10.1016/j.porgcoat.2020.105598
[18] Hassan A.G., Yajid M.M., Saud S.N. *et al*.: *Surface and Coatings Technology* **2020**, *401*, 126257. https://doi.org/10.1016/j.surfcoat.2020.126257
[19] Chen M., Wang G.C., Yang W.Q. *et al*.: *ACS Applied Materials and Interface*s **2019**, *11*(*45*), 42156. https://doi.org/10.1021/acsami.9b14316
[20] Chen M., Wang G.C., Shao L.L. *et al*.: *ACS Applied Materials and Interfaces* **2018**, *10*(*37*), 31208. https://doi.org/10.1021/acsami.8b08489
[21] Chen M., Zhao G., Shao L.L. *et al*.: *Chemistry of Materials* **2017**, *29*(*22*), 9680. https://doi.org/10.1021/acs.chemmater.7b03385
[22] Chen M., Shao L.L., Lv X.W. *et al*.: *Chemical Engineering Journal* **2020**, *390*, 124633. https://doi.org/10.1016/j.cej.2020.124633
[23] Janudin N., Abdullah N., Yasin F.M. *et al*.: *ZULFAQAR Journal of Defence Science, Engineering and Technology* **2018**, *1*(*2*). https://zulfaqarjdset.upnm.edu.my/index.php/zjdset/article/view/7
[24] Janudin N., Abdullah N., Wan Yunus W.M. *et al*.: *Journal of Nanotechnology* **2018**, article ID 2107898. https://doi.org/10.1155/2018/2107898
[25] Maity D., Rajavel K., Kumar R.T.: *Sensors and Actuators B: Chemical* **2018**, *261*, 297. https://doi.org/10.1016/j.snb.2018.01.152
[26] Schroeder V., Savagatrup S., He M. *et al*.: *Chemical Reviews* **2018**, *119*(*1*), 599. https://doi.org/10.1021/acs.chemrev.8b00340
[27] Kasim N.A., Abdullah N., Yasin F.M. *et al*.: *Materials Today: Proceedings* **2019**, *19*, 1459. https://doi.org/10.1016/j.matpr.2019.11.169
[28] Norizan M.N., Zulaikha N.S., Norhana A.B. *et al*.: *Polimery* **2021**, *66*(*3*), 175. https://doi.org/10.14314/polimery.2021.3.3
[29] Nurazzi N.M., Harussani M.M., Zulaikha N.S. *et al*.: *Polimery* **2021**, *66*(*2*), 85. https://doi.org/10.14314/polimery.2021.2.1
[30] Yahya M.S., Ismail M.: *The Journal of Physical Chemistry C* **2018**, *122*(*21*), 11222. https://doi.org/10.1021/acs.jpcc.8b02162
[31] Mananghaya M., Yu D., Santos G.N., Rodulfo E.: *Scientific Reports* **2016**, *6*(*1*), 1. https://doi.org/10.1038/srep27370
[32] Park S., Gupta A.P., Yeo S.J. *et al*.: *Nanomaterials* **2018**, *8*(*6*), 378. https://doi.org/10.3390/nano8060378
[33] Song Y., Li J., Wu Q. *et al*.: *Journal of Alloys and Compounds* **2020**, *816*, 152648. https://doi.org/10.1016/j.jallcom.2019.152648
[34] Ma P.C., Siddiqui N.A., Marom G., Kim J.K.: *Composites Part A: Applied Science and Manufacturing* **2010**, *41*(*10*), 1345. https://doi.org/10.1016/j.compositesa.2010.07.003
[35] Mohd Saidi N., Norizan M.N., Abdullah N. *et al*.: *Nanomaterials* **2022**, *12*(*7*), 1071. https://doi.org/10.3390/nano12071071
[36] Rubel R.I., Ali M.H., Jafor M.A., Alam M.M.: *AIMS Materials Science* **2019**, *6*(*5*), 756. https://doi.org/10.3934/matersci.2019.5.756
[37] Sabet S.M., Mahfuz H., Terentis A.C. *et al*.: *Journal of Materials Science* **2018**, *53*(*12*), 8963. https://doi.org/10.1007/s10853-018-2182-y
[38] Nurazzi N.M., Sabaruddin F.A., Harussani M.M. *et al*.: *Nanomaterials* **2021**, *11*(*9*), 2186. https://doi.org/10.3390/nano11092186
[39] Husain A., Shariq M.U., Mohammad F.: *Materialia* **2020**, *9*, 100599. https://doi.org/10.1016/j.mtla.2020.100599
[40] Zhao Y.L., Stoddart J.F.: *Accounts of Chemical Research* **2009**, *42*(*8*), 1161. https://doi.org/10.1021/ar900056z
[41] Li X., Zhu Z., Wang T. *et al*.: *Composites Communications* **2019**, *12*, 128. https://doi.org/10.1016/j.coco.2019.01.009
[42] Husain A., Ahmad S., Mohammad F.: *Materials Chemistry and Physics* **2020**, *239*, 122324. https://doi.org/10.1016/j.matchemphys.2019.122324
[43] Rathore P., Negi C.M., Yadav A. *et al*.: *Optik* **2018**, 160, 131. https://doi.org/10.1016/j.ijleo.2018.01.092
[44] Saini V., Li Z., Bourdo S. *et al*.: *The Journal of Physical Chemistry C* **2009**, *113*(*19*), 8023. https://doi.org/10.1021/jp809479a
[45] Mescoloto A.D., Pulcinelli S.H., Santilli C.V., Gonçalves V.C.: *Polímeros* **2014**, *24*, 25.

http://dx.doi.org/10.4322/polimeros.2014.04
[46] Karim M.R.: *Journal of Nanomaterials* **2012**, article ID 174353.
https://doi.org/10.1155/2012/174353
[47] Husain A., Ahmad S., Mohammad F.: *Polymers and Polymer Composites* **2021**, *29*(*6*), 605.
https://doi.org/10.1177/0967391120929079
[48] Agbolaghi S.: *Iranian Journal of Materials Science and Engineering* **2020**, *17*(2), 39.
https://doi.org/10.22068/ijmse.17.2.39
[49] Mahakul P.C., Sa K., Subramanyam B.V. *et al*.: *Journal of Materials Science* **2018**, *53*(*11*), 8151.
https://doi.org/10.1007/s10853-018-2161-3
[50] Das A.K., Bhowmik R., Meikap A.K.: *AIP Advances* **2017**, *7*(*4*), 045110.
https://doi.org/10.1063/1.4980051
[51] Tai C.K., Yeh P.L., Chang C.C. *et al*.: *Research on Chemical Intermediates* **2014**, *40*(*6*), 2355.
https://doi.org/10.1007/s11164-014-1612-y
[52] Norizan M.N., Mohamed R.: *Jurnal Teknologi* **2017**, *79*(2).
https://doi.org/10.11113/jt.v79.8436
[53] Riaz A., Usman A., Faheem M. *et al*.: *International Journal of Electrochemical Science* **2017**, *12*(*3*), 1785.
https://doi.org/10.20964/2017.03.20
[54] Rasheed H.K., Kareem A.A.: *Journal of Optical Communications* **2021**, *42*(*1*), 25.
https://doi.org/10.1515/joc-2018-0024
[55] Bafandeh N., Larijani M.M., Shafiekhani A. *et al*.: *Chinese Physics Letters* **2016**, *33*(*11*), 117801.
https://doi.org/10.1088/0256-307X/33/11/117801
[56] Swamy N.K., Sandeep S., Santhosh A.S.: *Indian Journal of Advances in Chemical Science S2* **2017**, *6*, 9.
DOI:10.22607/IJACS.2017.S02002
[57] Saleh M.A., Jawad M.K.: *IOP Conference Series: Materials Science and Engineering* **2020**, *928*, 072140.
https://doi.org/10.1088/1757-899X/928/7/072140
[58] Kadem B., Alfahed R.F., Al-Asadi A.S., Badran H.A.: *Optik* **2020**, *204*, 164153.
https://doi.org/10.1016/j.ijleo.2019.164153
[59] Anyaegbunam F.N., Augustine C.: *Digest Journal of Nanomaterials and Biostructures* **2018**, *13*, 847.

Received 7 IV 2022.

Rapid Communications

Przypominamy Autorom, że publikujemy artykuły typu **Rapid Communications – prace oryginalne wyłącznie w języku angielskim** (o objętości 4–5 stron maszynopisu z podwójną interlinią, zawierające 2–3 rysunki lub 1–2 tabele), którym umożliwiamy szybką ścieżkę druku (do 3 miesięcy od chwili ich otrzymania przez Redakcję). Artykuł należy przygotować wg wymagań redakcyjnych zamieszczonych we wskazówkach dla P.T. Autorów.

* * *

We remind Authors that we publish articles of the **Rapid Communications** type – **the original papers, in English only** (with a volume of 4-5 pages of double-spaced typescript, containing 2–3 figures or 1–2 tables), which allow a fast print path (up to 3 months from when they are received by the Editorial Board). The article should be prepared according to the editorial requirements included in the Guide for Authors.